AGU PUBLICATIONS

Journal of Advances in Modeling Earth Systems

RESEARCH ARTICLE
10.1002/2015MS000548

Key Points:
- Introduces the concept of two, rather than one, ranges of scales to model the boundary layer
- Seamlessly combine the "local" and the "nonlocal" approaches to boundary layer modeling
- Physically based formulation used to counteract some of the numerical artifacts

Correspondence to:
R. Bhattacharya,
ritthik.bhattacharya@jpl.nasa.gov

Citation:
Bhattacharya, R., and B. Stevens (2016), A two Turbulence Kinetic Energy model as a scale-adaptive approach to modeling the planetary boundary layer, *J. Adv. Model. Earth Syst.*, *8*, 224–243, doi:10.1002/2015MS000548.

Received 15 SEP 2015
Accepted 18 JAN 2016
Accepted article online 21 JAN 2016
Published online 20 FEB 2016

A two Turbulence Kinetic Energy model as a scale-adaptive approach to modeling the planetary boundary layer

Ritthik Bhattacharya[1,2,3] and Bjorn Stevens[1]

[1]Max Planck Institute for Meteorology, Hamburg, Germany, [2]International Max Planck Research School, Max Planck Institute for Meteorology, Hamburg, Germany, [3]Division of Geological and Planetary Sciences, California Institute of Technology, Pasadena, California, USA

Abstract A two Turbulence Kinetic Energy (2TKE) model is developed to address the boundary layer "grey zone" problem. The model combines ideas from *local* and *nonlocal* models into a single energetically consistent framework. By applying the Reynolds averaging to the large eddy simulation (LES) equations that employ Deardorff's subgrid TKE, we arrive at a system of equations for the boundary layer quantities and two turbulence kinetic energies: one which encapsulates the TKE of large boundary-layer-scale eddies and another which represents the energy of eddies subgrid to the vertical grid size of a typical large-scale model. These two energies are linked via the turbulent cascade of energy from larger to smaller scales and are used to model the mixing in the boundary layer. The model is evaluated for three dry test cases and found to compare favorably to large eddy simulations. The usage of two TKEs for mixing helps reduce the dependency of the model on the vertical grid scale as well as on the free tropospheric stability and facilitates a smoother transition from convective to stable regimes. The usage of two TKEs representing two ranges of scales satisfies the prerequisite for modeling the boundary layer in the "grey zone": an idea that is explored further in a companion paper.

1. Introduction

Boundary layer parameterizations in large-scale models have usually been designed on the basis of the assumption that the entirety of boundary layer processes is subgrid, although the vertical structure of the boundary layer mean profiles might be resolved, at least away from the entrainment and the surface layers. Large eddy simulations (LESs), on the other hand, are designed to resolve much of the energy-containing boundary-layer-scale eddies and model the locally homogeneous isotropic turbulence that remains unresolved, via the LES-subgrid schemes. With increasing computational power, the grid size of global and regional models in which boundary layers are traditionally parameterized is becoming smaller. For instance, the German weather service runs a convection-resolving model, with a horizontal grid spacing of 2.8 km to perform short-term forecasts [*Baldauf et al.*, 2011]. Hence, they are beginning to resolve some of the boundary-layer-scale processes but not yet to the degree of LES models.

Wyngaard [2004] referred to this intermediate scale, wherein boundary layer turbulence is not well resolved, but nor is the grid scale so large that it allows one to use Reynolds-averaged approximations, as "Terra incognita," others refer to this as the "grey zone." Modeling of partially resolved boundary layer circulations at these grid scales requires parameterizations that are aware of the size of the scales they resolve, as well as the depth of the boundary layer as a whole. This allows the parameterization to "know" which part of the processes are resolved and which parts are subgrid for a given grid size. The present paper presents the derivation and initial tests of a model designed to work both at the large-scale limit of contemporary global models as well as the LES limit of grid sizes. The idea is that such a model should also behave reasonably on intermediate scales, i.e., within the "grey zone." To work in both the LES and the large-scale limits described above, our model is designed to be aware of two scales: the boundary layer depth and the size of the vertical mesh. In this paper, the derivation of the model and tests of the model in the large-scale limit are presented. In the companion paper (R. Bhattacharya and B. Stevens, Modeling the planetary boundary layer in the "grey zone" using a two Turbulence Kinetic Energy model, submitted to *Journal of Advances in Modeling Earth Systems*, 2015), we present results from the model imbedded in an anelastic flow-solver run at different horizontal resolutions so as to demonstrate the adequacy of the model across the "grey zone."

The basic idea we explore is the usage of two turbulence kinetic energies (and corresponding length scales) each representing a range of scales of subgrid mixing within the boundary layer. Usually, models of the planetary boundary layer (PBL) explicitly adopt a single, or master, length scale, which is assumed to play the dominant role inside the boundary layer. For example, many PBL models represent the vertical heat fluxes inside the boundary layer as

$$\overline{\Theta' w'} = -K_h \left(\frac{\partial \bar{\Theta}}{\partial z} \right). \tag{1}$$

Here Θ and w are the potential temperature and the vertical wind velocity, respectively (overbar and prime notation denote Reynolds averaging and fluctuations therefrom). K_h on the right-hand side (RHS) thus represents an eddy diffusivity, which can be described as the product of a turbulence velocity and a length scale. Different approaches have been developed to model these two constituent quantities. In some approaches, the velocity scale is derived from the local turbulence kinetic energy within a grid box and the local stability [*Bretherton and Park*, 2009; *Brinkop and Roeckner*, 1995]. Length scales can also be defined locally [*Blackadar*, 1962; *Grenier and Bretherton*, 2001] or may take the height within the boundary layer, or the boundary layer depth itself into account [*Troen and Mahrt*, 1986]. In other models, a nonlocal approach uses gross boundary layer properties like its depth and the surface buoyancy flux [*Troen and Mahrt*, 1986]; see also *Large et al*. [1994]. In general, the *local* description for the velocity and the length scale works well for stable to near-neutral boundary layers which have smaller turbulent structures that are more influenced by the local stability, whereas the *nonlocal* schemes often performs better in convective conditions with larger boundary-layer-scale turbulent structures.

Attempts have been made to combine these two descriptions: either using switching between these two descriptions depending on scenarios [*Lock et al*., 2000] or by a hybrid approach which uses two different modes of mixing within a single scheme. An important and influential example of the hybrid approach is the eddy diffusivity mass flux (EDMF) model as introduced by *Siebesma et al*. [2007]. The EDMF model uses eddy diffusivity to model the local mixing and introduces a mass flux (like the type clouds are modeled with, for example by *Tiedke* [1989]) to model the nonlocal buoyancy driven plumes. However, it does not formally relate the eddies that carry on the nonlocal transport to those that perform the local mixing, which is the case in reality since the former drive the later through the turbulence cascade [*Kolmogorov*, 1991]. The present work draws inspiration from the EDMF model and seeks to fill this gap in the simplest possible framework.

The key focus of this 2TKE model development has been to address the scale awareness of the boundary layer schemes and to utilize the current understanding of boundary layer dynamics to guide our effort. In the past years, a main focus has been in the development of better models of boundary layer turbulence. Examples include second-moment closures [*Mellor and Yamada*, 1974; *Bougeault*, 1981a, 1981b] that solve for the second moments prognostically and thus can better represent the interplay between the turbulence and the mean profile. More recently a different approach, assumed PDF models [*Lappen and Randall*, 2001a, 2001b, 2001c; *Golaz et al*., 2002a, 2002b], has been adopted. These models aim to physically link boundary layer models which solve for means and variances, and cloud models that use probability density functions to determine cloudiness, updraft area fraction, etc. These models assume joint PDFs of moist-conserved variables like liquid water potential temperature and total water content as well as of the vertical velocity. They then solve for evolution equations for the means, variances and covariances of these variables to describe the evolution of these PDFs in space and time. Our ideas are not meant to supplant these approaches, nor do they claim to more accurately represent the boundary layer for any particular implementation. Rather our focus is on the development of a framework for modeling boundary layer turbulence flexibly and dynamically on grids with different resolution.

Our aim in developing the 2TKE model is to create a model that can reproduce LES results in the limit of LES grid sizes while at the same time represent the boundary layer physically in large-scale model applications. To do so, we start with the LES equations and apply boundary layer approximations that are common place in the derivation of parameterizations of Reynolds-averaged models [*Mellor and Yamada*, 1974]. Such an approach introduces two turbulence energies: one (called the large TKE) representing the energy of eddies ranging from the horizontal grid size to the vertical grid size and the other (called the small TKE) representing the energy of eddies subgrid to the vertical grid size. We endeavor to link these to one another,

and the mean flow, in a physical manner. In doing so, we use to our advantage both the local and the nonlocal approaches for modeling turbulence. As we demonstrate in the companion paper (Bhattacharya and Stevens, submitted manuscript, 2015) (*where we implement this scheme in a large eddy simulation model*), the resulting model working in these two limits can be physically tuned to also work reasonably in the range of grid sizes in between. This is aided by the fact that in this intermediate range of grid sizes, the small TKE continues to operate fully while the large TKE needs to be blended to account for the fact that some of the large eddies are being gradually resolved by the horizontal grid.

The paper is organized as follows: section 2 presents the major steps in the derivation of the 2TKE model and provides a rationalization for the assumptions necessary to close the system of equations we derive. Comparison with two currently used PBL schemes: a rather crude TKE scheme (an example of local parameterization) as used in ECHAM [*Brinkop and Roeckner*, 1995] and the *K*-profile parameterization (a nonlocal scheme) found in many other models [*Troen and Mahrt*, 1986] is presented in section 3. Finally, perspectives and conclusions are presented in section 4.

2. 2TKE Model Description

Before presenting a formal derivation of our model, we first give an overview of the main approach. Conventions for the notation are presented section 2.1 and the formal derivation of the 2TKE model is presented thereafter. As discussed in section 1, it is desired that the model reduces to a traditional LES representation in the limit that the grid spacing is much smaller than the depth, h, of the PBL. Hence, we begin with the LES equation set for which the subgrid-scale fluxes are modeled using a small-scale turbulence kinetic energy [*Deardorff*, 1980]. The LES equations are then averaged analogous to what is done when deriving the Reynolds-averaged Navier Stokes (RANS) models, i.e., assuming that the energy-containing eddies, whose scale is of order h, are much smaller than the horizontal grid spacing [e.g., see *Mellor and Yamada*, 1974]. The vertical grid is initially assumed to be of the order of what one finds in LES, but this assumption will later be relaxed. For this presentation, only a dry incompressible fluid is considered. The PBL equations derived in this manner differ from typical PBL equations in one key aspect: instead of a single TKE, two energies emerge: a large-scale TKE that accounts for eddy sizes from the boundary layer scale to the vertical grid size and a small-scale TKE which accounts for eddies which are subgrid to the vertical grid size.

These equations require a closure assumption for the large-scale average of the LES-subgrid stresses (that occur in the original LES equations) as well as the Reynolds stresses arising from larger, but still subgrid, eddies. A down-gradient approximation is made in both cases, using the small-scale TKE and the large-scale TKE, respectively. The former is restricted to work on a length scale proportional to the vertical grid size as well as in regions of strong stratification, as for instance within the entrainment zone capping convective boundary layers. Within such an entrainment zone, small eddies entrain warmer air from free troposphere into the boundary layer. The latter on the other hand, works on the scale of the boundary layer height and hence is modeled in a *nonlocal* fashion with a *K*-profile, taking into account the free tropospheric stability as well as the fact that the small-scale energy contributes to the mixing especially at the surface and the entrainment zones. The sum of the large-scale and the small-scale energies is independent of the vertical grid size, and at the same time dissipation of large energy acts as a source of the small-scale energy (through the energy cascade) [*Kolmogorov*, 1991]. These two constraints relate the dissipation scale of the large-scale energy to that of the small-scale energy (which is tied to the vertical grid size) and help the model deal more flexibly and consistently with insufficient vertical resolution with regards to the mean structure of the entrainment layer.

Thus, in this manuscript, we derive the 2TKE model and use its implementation in a single-column setup to explore its properties in the limit of large horizontal grid sizes. In the companion paper (Bhattacharya and Stevens, submitted manuscript, 2015), we implement the 2TKE model in a large eddy simulation setup which allows us to extend it and explore its properties in the horizontal "grey zone."

2.1. Derivation of New Set of PBL Equations

To simplify the subsequent presentation, a few notational conventions as applicable to a generic variable ϕ of an unfiltered fluid field are first introduced. Solving for the fluid field in an LES model with grid size $\Delta \ll h$ yields

$$\phi = \Phi + \phi*, \tag{2}$$

where Φ is the LES resolved field (i.e., scales greater than Δ) and $\phi*$ represents the fluctuations smaller than Δ. The LES volume average, from which the LES resolved field is derived, is assumed to satisfy the properties of a Reynolds average. Now Φ can be decomposed into an average over a large horizontal grid box typical of a current global NWP or climate model (this average is equivalent to the Reynolds average and will be referred to as the large-scale average or the Reynolds average henceforth) and a Reynolds-subgrid fluctuation:

$$\Phi = \overline{\Phi} + \Phi'. \tag{3}$$

The Reynolds average of the LES resolved field should, in theory, be identical to the Reynolds average of the unfiltered fluid field from which the LES resolved fields have been derived. Thus,

$$\overline{\Phi} = \overline{\phi}. \tag{4}$$

The subgrid fluctuations differ however as they do not include fluctuations on scales smaller than Δ.

2.1.1. Equations for LES-Filtered Variables

The LES equations for the velocity vectors can be written as

$$\frac{\partial U_i}{\partial t} = -U_k \frac{\partial U_i}{\partial x_k} - c_p \Theta_0 \frac{\partial P}{\partial x_i} + \frac{g\Theta''}{\Theta_0}\delta_{i3} + f_j(U_k - U_{g,k})\epsilon_{ikj} - \frac{\partial \tau_{ik}}{\partial x_k}. \tag{5}$$

Here tensor notation is used, so that U_i denotes the three components of the LES-filtered velocity vector field, (U_1, U_2, U_3), alternatively (U, V, W). The subscript g refers to the geostrophic component. The independent spatial coordinates are given by $x_i = (x_1, x_2, x_3)$, alternatively (x, y, z). Repeated indices represent Einstein summation. The left-hand side represents the rate of change of LES velocity field. The terms on the RHS represent advection of specific momentum, the gradient of the ageostrophic pressure, P, a buoyancy term, the Coriolis acceleration (f being the Coriolis parameter) and the divergence of LES-subgrid stresses ($\tau_{ik} = \langle u_i^* u_k^* \rangle$), respectively. In the above, the double prime is used in the definition of the buoyancy term to denote deviations from the horizontal averages, and angle brackets, for notational clarity, denote averaging over the LES grid, so that $\Phi = \langle \phi \rangle$.

For potential temperature (Θ), in the absence of diabatic forcings, the evolution equation reads

$$\frac{\partial \Theta}{\partial t} = -U_k \frac{\partial \Theta}{\partial x_k} - \frac{\partial \gamma_k}{\partial x_k}. \tag{6}$$

γ_k represents the LES-subgrid flux of potential temperature, $\gamma_k = \langle \Theta^* u_k^* \rangle$.

For the LES (Deardorff) subgrid TKE, here denoted by e, we write the evolution equation as

$$\frac{\partial e}{\partial t} = -\frac{\partial (eU_k)}{\partial x_k} + \frac{\partial}{\partial x_k}\left(K_e \frac{\partial e}{\partial x_k}\right) - \tau_{ik}\frac{\partial U_i}{\partial x_k} + b - \frac{C_e}{l} e^{3/2}. \tag{7}$$

The terms on the right-hand side represent transport by advection; a diffusion term (with a diffusivity, K_e) that combines the effect of both the subgrid turbulence and the pressure-velocity covariances as a diffusion process of e; subgrid dissipation; buoyant production/destruction (b); and viscous dissipation (standard model following *Kolmogorov* [1991], with l being the dissipation length scale for e and C_e being a flow-dependent constant), respectively.

2.1.2. Derivation of Reynolds-Averaged Fields

Reynolds averaging of equation (5) (equation (4) implies $\bar{U} = \bar{u}$, $\bar{P} = \bar{p}$, etc.) yields

$$\frac{\partial \overline{u_i}}{\partial t} = -\overline{u_k}\frac{\partial \overline{u_i}}{\partial x_k} - \frac{\partial T_{ik}}{\partial x_k} - c_p \Theta_0 \frac{\partial \bar{p}}{\partial x_i} + \frac{g\overline{\Theta''}}{\Theta_0}\delta_{i3} + f_j(\overline{u_k} - U_{g,k})\epsilon_{ikj} - \frac{\partial \overline{\tau_{ik}}}{\partial x_k}, \tag{8}$$

where T_{ij} represents the Reynolds-subgrid stress

$$T_{ij} = \overline{U_i' U_j'}. \tag{9}$$

Because the double prime denotes differences from a horizontal average:

$$\overline{\Theta''}=0. \tag{10}$$

The Reynolds average of P as well as the advective (convective) tendency is resolved by the large-scale model. Also in a PBL model for large-scale applications, the vertical fluxes and gradients can be considered to be an order of magnitude larger than the horizontal ones [*Mellor and Yamada*, 1974]. This allows us to neglect the horizontal fluxes in the derivation of the 2TKE model, although formally they should be retained to preserve the correct LES limit, which implies that the Lagrangian acceleration of the Reynolds-averaged velocity can be described as follows:

$$\frac{D\overline{U_i}}{Dt}=\frac{\partial\overline{u_i}}{\partial t}+\overline{u_k}\frac{\partial\overline{u_i}}{\partial x_k}=-\frac{\partial T_{i3}}{\partial z}+f_j(\overline{u_k}-U_{g,k})\epsilon_{ikj}-\frac{\partial\overline{\tau_{i3}}}{\partial z}, \tag{11}$$

where D/Dt is defined implicitly as the advective derivative which follows the Reynolds-averaged flow. Similarly for Reynolds-averaged potential temperature field, we solve for

$$\frac{D\bar{\Theta}}{Dt}=-\frac{\partial\Gamma_3}{\partial z}-\frac{\partial\overline{\gamma_3}}{\partial z}, \tag{12}$$

where Γ_3 represents the Reynolds-subgrid-vertical potential temperature flux.

$$\Gamma_3=\overline{\Theta' W'}. \tag{13}$$

The difference between equations (5) and (8), again considering only the vertical fluxes describes the deviations from the Reynolds-averaged quantities, such that for the acceleration:

$$\begin{aligned}\frac{\partial U_i'}{\partial t} \quad &=-W'\frac{\partial\overline{u_i}}{\partial z}-\bar{w}\frac{\partial U_i'}{\partial z}-\frac{\partial(U_i'W'-\overline{U_i'W'})}{\partial z}\\ &-c_p\Theta_0\frac{\partial P'}{\partial x_i}+\frac{g\Theta''}{\Theta_0}\delta_{i3}+f_jU_k'\epsilon_{ikj}-\frac{\partial\tau_{i3}'}{\partial z}\end{aligned}. \tag{14}$$

Taking the Reynolds average of the inner product of the acceleration fluctuations with the velocity fluctuations and further assuming the Coriolis terms can be neglected within the boundary layer since hf/u_* is small (u_* is the surface friction velocity), yields an expression for E, the turbulence kinetic energy of eddies whose scales range from the vertical grid to the boundary layer depth (henceforth called the large-scale TKE):

$$\begin{aligned}\frac{\partial E}{\partial t}= \quad &-\overline{U'W'}\frac{\partial\bar{u}}{\partial z}-\overline{V'W'}\frac{\partial\bar{v}}{\partial z}-\bar{w}\frac{\partial E}{\partial z}-\frac{\partial}{\partial z}\overline{U_i'U_i'W'}\\ &-\frac{\partial\overline{\tau_{i3}'U_i'}}{\partial z}+\overline{\tau_{i3}'\frac{\partial U_i'}{\partial z}}+g\frac{\overline{W'\Theta''}}{\Theta_0}\end{aligned}. \tag{15}$$

Note that the pressure-velocity covariances redistribute the energy among the components but do not contribute to the total energy [*Rotta*, 1951], and so play no explicit role in equation (15).

The evolution equation for LES-subgrid TKE, e, has been given by equation (7). Partitioning the LES-subgrid TKE (e), the subgrid stress (τ_{ij}), and the buoyant production (b) into a Reynolds-averaged and a Reynolds-subgrid part ($e=\bar{e}+e'$, $\tau_{ij}=\overline{\tau_{ij}}+\tau_{ij}'$, $b=\bar{b}+b'$) yields

$$\begin{aligned}\frac{\partial(\bar{e}+e')}{\partial t} \quad &=-\frac{\partial((\bar{e}+e')(\overline{u_k}+U_k'))}{\partial x_k}+\frac{\partial}{\partial x_k}\left(K_e\frac{\partial(\bar{e}+e')}{\partial x_k}\right)\\ &-(\overline{\tau_{ik}}+\tau_{ik}')\frac{\partial(\overline{u_i}+U_i')}{\partial x_k}+\bar{b}+b'-\frac{C_e}{l}(\bar{e}+e')^{3/2}.\end{aligned} \tag{16}$$

Expansion of the dissipation term in the RHS leads to

$$\overline{(\bar{e}+e')^{3/2}}=\overline{\bar{e}^{3/2}}+\frac{3}{2}\overline{\bar{e}^{1/2}e'}+\frac{3}{8}\overline{\bar{e}^{-1/2}e'2}+hot\approx\bar{e}^{3/2}+\frac{3}{8}\bar{e}^{-1/2}\overline{e'2}, \tag{17}$$

wherein the approximation arises through the neglect of the higher order terms, denoted by *hot*. Substituting equation (17) into equation (16) and neglecting the horizontal terms as part of the boundary layer approximation yield an equation for the evolution of the Reynolds-averaged small-scale TKE:

$$\frac{\partial \bar{e}}{\partial t} = -\frac{\partial(\bar{e}\,\bar{w})}{\partial z} - \frac{\partial(\overline{e'W'})}{\partial z} + \frac{\partial}{\partial z}\left(K_e \frac{\partial \bar{e}}{\partial z}\right) - \overline{\tau_{i3}}\frac{\partial \overline{u_i}}{\partial z} - \overline{\tau'_{i3}\frac{\partial U'_i}{\partial z}} + \bar{b} - \frac{C_e}{l}\left(\bar{e}^{3/2} + \frac{3}{8}\bar{e}^{-1/2}\overline{e'2}\right) \tag{18}$$

Only flat surfaces are considered, i.e., $\bar{w}=0$ at the surface. This combined with incompressibility implies that $\bar{w}$ does not enter our set of PBL equations. Equations (11), (12), (15), and (18) thus represent the evolution equations for the horizontal wind components, the potential temperature, the large-scale TKE, and the Reynolds-averaged LES-subgrid TKE. These equations with the closures defined below define our 2TKE model.

2.1.3. Closure for the Subgrid Variances

The equations for E and $\bar{e}$ (i.e., equations (15) and (18)) contain multiple terms involving LES and/or Reynolds-subgrid fluxes. Closure of these LES-/Reynolds-subgrid fluxes implies approximating them using the LES-/Reynolds-resolved variables, respectively. For the most part, this can be accomplished using standard approaches as described below.

Like the diffusion of $\bar{e}$, the LES-subgrid stresses are related to the mean using a down-gradient model thus defining the diffusivity, K_e. Thus for example,

$$\tau_{13} = -K_e \frac{\partial U}{\partial z}. \tag{19}$$

K_e is assumed proportional to $\sqrt{\bar{e}}$ whose horizontal variations over the LES domain are neglected. The latter assumption also implies that $\overline{e'2}$ can be neglected in equation (18), since the horizontal variation of the e field has been neglected. Thus,

$$\overline{\tau'_{13}\frac{\partial U'}{\partial z}} = -K_e \overline{\frac{\partial U'}{\partial z}\frac{\partial U'}{\partial z}}, \tag{20}$$

which, being the product of a negative and a squared term, is always negative semidefinite. This means it always acts as a sink of E and a source for $\bar{e}$. Assuming, as the simplest case, that the Reynolds filter size is within the inertial subrange (though, for example, Wyngaard [2004] assume otherwise), this dissipation of E to $\bar{e}$ can be parameterized in the same manner as the dissipation of $\bar{e}$ itself, i.e.,

$$K_e \overline{\frac{\partial U'_i}{\partial z}\frac{\partial U'_i}{\partial z}} \approx \frac{C_E}{L} E^{3/2}. \tag{21}$$

From Kolgomorov theory, the constant of proportionality in the energy spectrum is the same throughout the inertial range:

$$C_e = C_E. \tag{22}$$

The length scale L (the dissipation length scale for E) may be parameterized as the Blackadar length [*Blackadar*, 1962]. As will be discussed later, this assumption can be relaxed based on the fact that the dissipation of E is a source of $\bar{e}$ according to the cascade of turbulence kinetic energy, but for now it is assumed that

$$L = \frac{\kappa z}{1 + \frac{\kappa z}{\lambda}}, \tag{23}$$

with λ denoting an asymptotic mixing length (taken as 150 m in some models) and κ being the Von Kármán constant. The dissipation length scale, l, of $\bar{e}$ is taken to be proportional to the vertical grid size, Δz of the model.

$$l = L\frac{\Delta z}{h}. \tag{24}$$

The other term that needs to be parameterized in equation (15) is $\overline{\frac{\partial \tau'_{i3} U'_i}{\partial z}}$. Using equation (19)

$$\frac{\partial \overline{\tau'_{i3} U'_i}}{\partial z} = -\frac{\partial \overline{K_e \frac{\partial U'_i}{\partial z} U'_i}}{\partial z} = -\frac{\partial}{\partial z}\left(K_e \frac{\partial E}{\partial z}\right), \tag{25}$$

the factor of 2/3 being absorbed in the definition of K_e.

Similarly, the vertical transport of Reynolds-averaged quantities by the Reynolds-averaged vertical velocity is modeled as

$$\overline{\Phi' W'} = -K_E \frac{\partial \bar{\Phi}}{\partial z}, \tag{26}$$

with K_E denoting the eddy viscosity of large (boundary layer scale) eddies. Thus, the equation for the Reynolds-averaged acceleration required by the large-scale model is

$$\frac{D\bar{u}_i}{Dt} = \frac{\partial}{\partial z}\left(K_E \frac{\partial \overline{u_i}}{\partial z}\right) - f_j(\overline{u_k} - V_{g,k})\epsilon ijk + \frac{\partial}{\partial z}\left(\overline{K_e \frac{\partial u_i}{\partial z}}\right). \tag{27}$$

It differs from the traditional form of this equation in that the vertical mixing is performed using two energies, represented in K_E and K_e, respectively. Closures require the additional assumption that fluctuations in K_e do not correlate with fluctuations in $\partial \overline{u_i}/\partial z$ across the grid scale of the large-scale model. With this final assumption, we arrive at a closed set of PBL equations which are presented below.

2.2. New Set of PBL Equations

Based on the above arguments, the 2TKE model can be written as

$$\frac{D\overline{u_i}}{Dt} = \frac{\partial}{\partial z}\left((K_E + K_e)\frac{\partial \overline{u_i}}{\partial z}\right) - f_j(\overline{u_k} - V_{g,k})\epsilon_{ijk}, \tag{28}$$

$$\frac{D\bar{\theta}}{Dt} = \frac{\partial}{\partial z}\left(P_r(K_E + K_e)\frac{\partial \bar{\theta}}{\partial z}\right), \tag{29}$$

$$\begin{aligned}\frac{\partial E}{\partial t} = {} & K_E\left(\left(\frac{\partial \bar{u}}{\partial z}\right)^2 + \left(\frac{\partial \bar{v}}{\partial z}\right)^2\right) + \frac{\partial}{\partial z}\left(K_E \frac{\partial E}{\partial z}\right) \\ & + \frac{\partial}{\partial z}\left(K_e \frac{\partial E}{\partial z}\right) - \frac{C_E}{L}E^{3/2} - \frac{gP_r K_E}{\Theta_0}\frac{\partial \bar{\theta}}{\partial z}\end{aligned} \tag{30}$$

$$\frac{\partial \bar{e}}{\partial t} = \frac{\partial}{\partial z}\left((K_E + K_e)\frac{\partial \bar{e}}{\partial z}\right),$$

$$+ K_e\left(\left(\frac{\partial \bar{u}}{\partial z}\right)^2 + \left(\frac{\partial \bar{v}}{\partial z}\right)^2\right) + \frac{C_E}{L}E^{3/2} + \bar{b} - \frac{C_e}{l}\left(\bar{e}^{3/2}\right). \tag{31}$$

In these equations, the Prandtl number (P_r), i.e., the ratio of the eddy diffusivity to the eddy viscosity, has been introduced. It is assumed to be similar for mixing via the boundary layer scale and the LES-subgrid eddies. In summary, the system consists of five governing equations instead of the usual four. The additional one is for Reynolds-averaged LES-subgrid TKE ($\bar{e}$). The governing equations for wind velocity and potential temperature require two separate eddy viscosities (diffusivities), one for boundary-layer-scale eddies (K_E) and the other for smaller isotropic eddies (K_e). This differs from the normal approach to PBL modeling wherein only a single eddy viscosity (diffusivity), which encapsulates the entire range of eddies within the boundary layer, is acknowledged.

When this new set of PBL equations is taken to the limit that the Reynolds average tends to an LES filter (the large-scale energy-containing eddies getting resolved meaning also that K_E tending to zero), this set reduces to the LES equation set we started with, with one key difference: the original set modeled small-scale subgrid horizontal fluxes alongside the vertical fluxes while this new derived set models only the vertical fluxes (this difference comes due to the boundary layer approximations we applied early on in our derivation of the PBL equations). This difference could and should be addressed in a more general formulation of the approach, but because our focus is on the "grey zone," wherein we continue to assume that these terms play a more minor role, we continue to neglect them here. In the companion paper (Bhattacharya and Stevens, submitted manuscript, 2015), we explore the region of grid sizes where this three dimensionality of fluxes begin to become essential.

We can note that to solve for these equations require modeling of the diffusivities (K_E and K_e) as well as the dissipation of E and $\bar{e}$. Next we present our methodology for accomplishing that.

2.3. Modeling of the Diffusion and the Dissipation

2.3.1. Modeling K_e, the Small-Eddy Diffusivity

Mixing by small-scale eddies is represented by K_e in the 2TKE model. It is modeled such that it plays a substantial part in mixing near the surface as well as in the entrainment zone. In the entrainment zone, it is designed to mix the warmer air from above the boundary layer into the layer, following for instance, the theoretical arguments of *Mellado et al*. [2014]. The diffusivity also physically incorporates the vertical grid size, and in so doing can help minimize some of the deleterious effects of insufficient vertical resolution.

K_e is defined (similar to current large-scale models) as

$$K_e = l_{\text{mix}}\sqrt{\bar{e}}, \tag{32}$$

where l_{mix} represents the length scale of mixing via the smaller eddies. With l_{mix} proportional solely to the vertical grid size, E causes most of the mixing throughout the boundary layer, i.e., the role of $\bar{e}$ insignificant. To make this scheme more grid independent, we introduce another length scale: the depth of the inversion layer, to account for the fact that this layer is often unresolved, and thus to allow $\bar{e}$ to account, as it should, for the mixing in this region. The idea is that the mixing which causes entrainment at the top of the boundary layer is carried out by the smaller eddies which includes some influence of the stability of the region (since the formulation of $\bar{e}$ involves local grid point variables). This is somewhat different from the EDMF formulation by *Siebesma et al*. [2007], wherein the *local* scheme acts predominantly in the surface layer, whereas the *nonlocal* scheme has the major contribution within the mixed layer and within the entrainment zone (entrainment, in this view point, is carried out by larger eddies originating at the surface and penetrating the stable region above the mixed layer). In our model, these large eddies provide one source term for $\bar{e}$ which actualize the mixing.

Taking the above into consideration, l_{mix} is formulated as

$$l_{\text{mix}} = \left[\frac{\kappa(h-z)}{1+\frac{\kappa(h-z)}{\Lambda}}\right]\frac{A}{\Delta z^{1/2}}. \tag{33}$$

The term in the square brackets on the right-hand side represents the influence of the entrainment zone in mixing (similar to what *Blackadar* [1962] does for the surface scales). Here Λ is the depth of entrainment zone. Λ is calculated per time step as the difference between the boundary layer depth and the mixed layer depth. The mixed layer depth is approximated as the model level height through which the gradient of the potential temperature remains small. Outside the entrainment zone (i.e., when $h-z > \Lambda$), the denominator of the term in square bracket is set at a constant value of $(1+\kappa)$ to ensure that the mixing contribution from $\bar{e}$ does not go below a certain limit.

For just this first term in the formulation, above experiments at very coarse grids show that K_e performs excessive mixing at the top of the boundary layer, leading to unrealistic growth of the boundary layer. Hence, the second term in the RHS is used as a numerical correction factor (A is a constant with dimensions of $m^{-1/2}$: this is set by the finest-grid solutions, that is considered to be the "true solution"). This is justified because from the inertial range theory [*Kolmogorov*, 1991], $\bar{e}$ scales with $\Delta z^{2/3}$ and so the length scale should decrease such that the product does not increase unrealistically for coarse grids. In summary, our formulation for l_{mix} includes a contribution from the entrainment zone as well as the vertical grid size of the model.

2.3.2. Modeling K_E, the Large Eddy Diffusivity

The large eddy diffusivity is modeled such that the large-scale fluxes and profiles are reasonably represented, especially for the simple case of a convective boundary layer with constant surface fluxes.

By definition, E depends on the large-scale features of the boundary layer, rather than the specific thermodynamic and dynamic state at each model level. Hence, E_1 is introduced as the vertical average of E (details of the calculation of the PBL depth, h, are given in section 2.4):

$$E_1(t) = \frac{1}{h(t)}\int_0^{h(t)} E(z,t)\,\mathrm{d}z. \tag{34}$$

The evolution equation for E_1 can be derived by integrating the evolution equation for E (section 2.2):

$$\frac{\mathrm{d}(hE_1(t))}{\mathrm{d}t}=\int_0^{h(t)}\frac{\partial E(z,t)}{\partial t}\mathrm{d}z+E(h,t)\frac{\mathrm{d}h(t)}{\mathrm{d}t}. \tag{35}$$

The integral in equation (35) can be estimated from the bulk properties of the boundary layer (assuming logarithmic and linear profiles for velocity and flux profiles, respectively). The discretized equation thus becomes

$$\begin{aligned}\frac{(hE_1)^{n+1}-(hE_1)^n}{\Delta t}&=\frac{0.4g(h^{n+1})\overline{w'\theta'}_0}{\Theta_0}+(\overline{E'w'}_0-\overline{E'w'}_h)\\&+\frac{w_c{u_*}^2}{\kappa}\left((\ln\lambda-\ln z_0)+\frac{\lambda^2-{z_0}^2}{2h^2}-\frac{2(\lambda-z_0)}{h}\right)\\&-C_E{E_1}^{3/2}\left(\frac{\ln(h^{n+1})-\ln(z_0)}{\kappa}+\frac{h^{n+1}-z_0}{\lambda}\right)+E(h^{n+1})\frac{h^{n+1}-h^n}{\Delta t},\end{aligned} \tag{36}$$

where the superscript denotes the time level, z_0 represents the surface roughness length, and u_* represents the surface friction velocity. The terms on the RHS represent the contributions from the integrated buoyancy flux profile (the surface flux generates E, while E mixes the warm air from the entrainment zone into the mixed layer), the fluxes of E at the surface and the top of the boundary layer, the integrated momentum profile, the dissipation of E to $\bar{e}$ and the growth of the layer height.

The introduction of the large-scale energy, E_1, facilitates the definition of a convective velocity scale as

$$w_c=\sqrt{2E_1}. \tag{37}$$

Upon defining w_c, a profile is used to diagnose K_E, following the general approach of *Troen and Mahrt* [1986]:

$$K_E=\kappa w_c h\left(\frac{z}{h}\right)\left(1-\frac{z}{h}\right)^m. \tag{38}$$

In the present implementation of the 2TKE model, this exponent is made to factor in two considerations: one is the free tropospheric stability and the other, the contribution of K_e to mixing.

To explore the dependence of K_E on the free tropospheric stability (G), cases with constant surface flux and no shear as well as no K_e have been considered with different values of G. For the boundary layer height to be correctly predicted, for instance as compared to LES, the flux at the point of minimum buoyancy must be correctly predicted. This is because, in the absence of mass flux coming out of the boundary layer (by convection or large-scale convergences), the boundary layer growth depends on the fluxes according to

$$\frac{dh}{dt}=\frac{\overline{w'\theta'}_0-\overline{w'\theta'}_{\min}}{Gh}, \tag{39}$$

shown, for example, by *Deardorff* [1974]. The height of the boundary layer is inversely proportional to the square root of the stability the boundary layer grows into provided the surface flux is constant [*Deardorff*, 1974]. Thus, to achieve the correct boundary layer growth, the flux at the height of minimum buoyancy should be independent of the stability above. This is achieved by equating the value of K_E at the height of minimum buoyancy (which LES studies suggest to be at similar nondimensional height for all convective boundary layers) for two different values of lower free tropospheric stability, G_1 and G_2. Here we take this nondimensional height to be δ. Thus, we want to solve for the exponent m_2 to be used for free tropospheric stability of G_2 whence we know the exponent m_1 being used for free tropospheric stability of G_1. Thus,

$$\kappa(Q_0h_1)^{1/3}h_1(\delta)(1-\delta)^{m_2}=\kappa(Q_0h_2)^{1/3}h_2(\delta)(1-\delta)^{m_1}, \tag{40}$$

where Q_0 is the surface buoyancy flux and h_1 and h_2 are the boundary layer heights for initial stability of G_1 and G_2, respectively. To simplify the calculation, we approximate the convective velocity scale in this instance to be the standard Deardorff convective velocity [*Deardorff*, 1970]. That is

$$w_c\approx(hQ_0)^{1/3}. \tag{41}$$

Equation (40) implies

$$(h_1)^{4/3}(1-\delta)^{m_2}=(h_2)^{4/3}(1-\delta)^{m_1}. \tag{42}$$

Now since the ideal height of a convective boundary layer driven by constant surface flux is inversely proportional to the square root of the stability equation (42) implies

$$m_2=m_1+\frac{2}{3}\log_{1-\delta}\left(\frac{G_1}{G_2}\right). \tag{43}$$

This revised exponent helps ensure that K_E accounts for the mixing responsible for the correct growth of the convective boundary layer, irrespective of the degree of stratification of the layer into which the boundary layer is growing.

The second factor taken into consideration in devising the exponent m is the fact that K_e accounts for much of the mixing within the surface and the entrainment layers. Our approach is to find an exponent such that the total diffusivity due to both the energies matches the diffusivity if only E was contributing to the mixing. We do this matching at one third the boundary layer depth, a depth where the standard K [*Troen and Mahrt*, 1986] maximizes and where *Deardorff* [1980] suggests the maximum vertical subgrid-vertical velocity variance within a convective boundary layer. Hence,

$$l_{mix}|_{h/3}\sqrt{\bar{e}}+\kappa w_s h\frac{1}{3}\left(\frac{2}{3}\right)^{m_1}=\kappa w_s h\frac{1}{3}\left(\frac{2}{3}\right)^{m}. \tag{44}$$

At a height of $h/3$, l_{mix} from equation (33) (the denominator within the square bracket being $1+\kappa$ as noted above) becomes

$$l_{mix}=\left[\frac{2h\kappa}{3(1+\kappa)}\right]\frac{A}{\Delta z^{1/2}}. \tag{45}$$

We consider solutions employing a grid spacing of 10 m as the "true" solutions (setting the constant A to $\sqrt{10}$) and to keep the correction due to $\bar{e}$ to the length scale of E minimal, we consider a large value of $\Delta z=256$ m. This implies

$$l_{mix}=\left[\frac{2h\kappa}{3(1+\kappa)}\right]\frac{\sqrt{10}}{16}. \tag{46}$$

Now since $O(\bar{e})$ is approximately $O(E/10)$ or

$$\sqrt{\bar{e}}\approx\frac{w_s}{\sqrt{10}}, \tag{47}$$

it follows that

$$\begin{aligned}&\frac{0.5}{4(1+\kappa)}+\left(\frac{2}{3}\right)^{m_1}=\left(\frac{2}{3}\right)^{m}\\ &\Rightarrow m_1=\frac{log\left(\frac{2}{3}\right)^{m}-\frac{0.5}{4(1+\kappa)}}{log(\frac{2}{3})}.\end{aligned} \tag{48}$$

The consequences of these choices (with E performing most of the mixing in the mixed layer and $\bar{e}$ near the interfaces) are seen in the solutions for different test cases (section 3).

2.3.3. Modeling Dissipation to Get Consistent Energetics

Equation (20) shows that the dissipation of E leads to a production of $\bar{e}$. This can be conceptualized in terms of the energy cascade in which large-scale turbulent eddies cascades into smaller scales eddies, which eventually dissipate. Not only are the two energies connected by the cascade, the sum of E and $\bar{e}$ should be constant irrespective of vertical grid size of the host single-column model (Δz partitions the inertial range without changing its size or shape). Using these two constraints leads to a relation between the dissipation length scales of these two energies, which aids in a consistent treatment of the turbulence energy as a whole and improves the convergence of the model solutions at coarser grids.

Writing the evolution equations for the two energies in a symbolic form ($\mathcal{P}_g$ and $\mathcal{P}_l$ representing global and local production terms, respectively), we get

$$\frac{dE}{dt} = \mathcal{P}_g(w_c, u_*) - C_E \frac{E^{3/2}}{L} \tag{49}$$

and

$$\frac{d\bar{e}}{dt} = \mathcal{P}_l\left(\frac{\partial \bar{u}}{\partial z}, \frac{\partial \bar{\Theta}}{\partial z}\right) + C_E \frac{E^{3/2}}{L} - C_e \frac{\bar{e}^{3/2}}{l}. \tag{50}$$

Assuming steady solutions allows one to neglect the time derivatives. Given that the vertical grid size is substantially smaller than the boundary layer height implies that the local production of $\bar{e}$ in equation (50) ($\mathcal{P}_l$) may be neglected. This leads us to a dominant balance between the transfer of energy from E to $\bar{e}$ and the dissipation of e by viscosity:

$$C_E \frac{E^{3/2}}{L} \approx C_e \frac{\bar{e}^{3/2}}{l}. \tag{51}$$

Now because C_E and C_e are dependent on the flow and by similarity [*Kolmogorov*, 1991], the same, that implies

$$\frac{E^{3/2}}{L} = \frac{\bar{e}^{3/2}}{l}. \tag{52}$$

Now for all Δz, the sum of E and $\bar{e}$ should be constant, since Δz is essentially partitioning the inertial subrange into two parts. This implies

$$\bar{e} + E = \mathcal{E}. \tag{53}$$

Equations (52) and (53) imply that

$$\bar{e}\left(1 + \frac{L^{2/3}}{l^{2/3}}\right) = \mathcal{E}, \tag{54}$$

$\mathcal{E}$ being a constant. Thus, the length scale of dissipation of E to $\bar{e}$ (i.e., L) is related to the length scale of dissipation of $\bar{e}$ (i.e., l) which is proportional to Δz, as follows:

$$L = l(\mathcal{E}\bar{e})^{3/2}\left(1 - \frac{\bar{e}}{\mathcal{E}}\right)^{3/2}. \tag{55}$$

If the δz dependence of $\bar{e}$ is neglected, then L becomes proportional to l, which makes it proportional to Δz. This, however, is unphysical since the dissipation scales of L are well removed from Δz. Therefore, approximating that $\bar{e}$ is proportional to $(\Delta z)^{2/3}$ while $\mathcal{E}$ is proportional to $h^{2/3}$ (again taking inertial subrange into account), three different approximations to L can be formulated. The first one neglects the magnitude of e with respect to $\mathcal{E}$, the second takes a simple two term expansion of equation (55), while the third one takes four consecutive terms of the binomial expansion of the same:

$$L \approx \frac{hl}{\Delta z}, \tag{56}$$

$$L \approx \frac{hl}{\Delta z} - l, \tag{57}$$

$$L \approx l\left(\frac{h}{\Delta z} - \frac{3h^{1/3}}{2\Delta z^{1/3}} + \frac{3\Delta z^{1/3}}{8h^{1/3}} - \frac{\Delta z}{16h}\right). \tag{58}$$

Equation (56) leads to independence of L from Δz, which was originally the case. Equation (57) leads to

$$L \approx l\left(\frac{h}{\Delta z} - 1\right). \tag{59}$$

Equation (58) can be simplified to

$$L \approx \frac{hl}{\Delta z}\left(1 - c\frac{\Delta z^{4/3}}{h}\right). \tag{60}$$

The constant c is a dimensional quantity which is necessary to make the second term inside the bracket nondimensional. Equation (58), that is, reduction of the length scale of dissipation of E by a

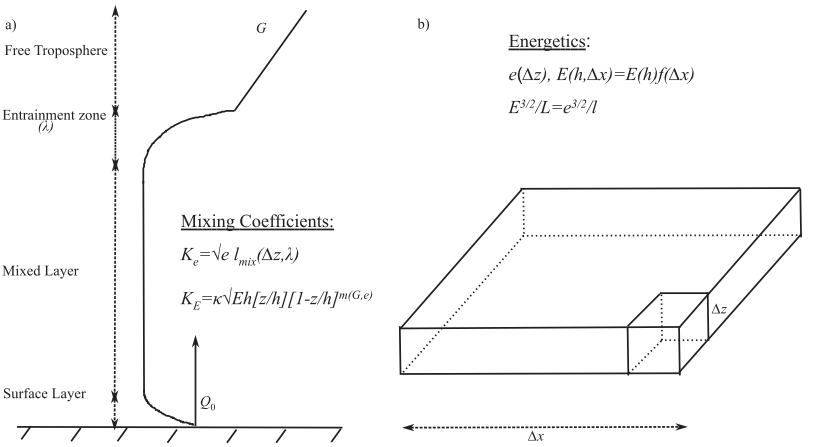

Figure 1. Schematic diagram outlining (a) the mixing formulations and (b) the energetics of the 2TKE model. The boundary layer depth is *h*.

term which has a slight superlinear exponent in Δz, leads to a significant reduction of vertical grid dependency of the solutions and as is shown in section 3, consistent energetics across a range of grid sizes.

Figure 1 summarizes the mixing and the energetic equations schematically. Figure 1a visualizes the mixing equations and shows how they incorporate the different aspects of the convective boundary layer as well as the vertical grid size into their formulations. Figure 1b rehashes the key aspects of the two turbulent kinetic energies for a NWP grid box with horizontal spacing of Δx and a vertical spacing of Δz. An LES grid box (of scale Δz in all three directions) is overlaid on this NWP grid box at the bottom left. Thus, $\bar{e}$ represents the NWP-grid-box-averaged LES-subgrid energy, while E represents the "remaining" turbulent kinetic energy within the NWP grid box. Note that for a finite horizontal grid size (Δx), the large TKE, E is a function of both the boundary layer depth as well as the horizontal grid size. This function (of Δx) has a value 1 for large-enough horizontal grid size (none of the large eddies resolved) and a value 0 for grid sizes tending to the LES grid size (entirety of the large eddies resolved). Since the current manuscript deals only with a single-column model (assumed infinite horizontal grid size), the function of horizontal grid size is not discussed. Designing this function is the key theme of the companion paper (Bhattacharya and Stevens, submitted manuscript, 2015).

2.4. Depth Diagnosis of the PBL

Two boundary layer depth diagnosis procedures have been employed. The first one, called the gradient method [*Sullivan and Patton*, 2011], is used when a purely convective boundary layer without shear has been studied. This method calculates the depth of the boundary layer at the height where the vertical slope of the potential temperature profile is maximum. However, in the presence of shear, another method, called the parcel method, has been used [following *Troen and Mahrt*, 1986]. This method starts by calculating an initial estimate of the boundary layer height, such that a parcel of air having the same properties as the surface exceeds a certain critical Richardson number (Ri_{cr}) at that height. This initial estimate allows the calculation of a convective velocity scale, which along with the surface friction velocity gives an estimate of the velocity scale at the surface, w_s (similar to equation (37)). This velocity scale allows the introduction of the temperature excess ($\Delta\theta$), such that

$$\Delta\theta = \frac{D\overline{w'\theta'}(0)}{w_s}. \tag{61}$$

The (new)boundary layer height is then calculated as the height where a parcel with temperature of the first model level plus $\Delta\theta$ exceeds Ri_{cr}. This method has been used in all the cases with a mean wind. In a pure dry convective boundary layer case with no wind, the gradient scheme has been used.

Table 1. Case Description

Case	Boundary Condition	Initial Condition	Boundary Layer Height Diagnosis
CBL1	1. Surface heat flux = 0.05 K m s^{-1} 2. Full slip condition	1. Lapse rate = 6 K km^{-1} starting at 299 K near surface 2. Wind speed = 10 m s^{-1} = geostrophic wind	Parcel method
CBL	Surface heat flux = 0.05 K m s^{-1}	1. Lapse rate = 6 K km^{-1} starting at 299 K near surface 2. No wind	Gradient method
SBL	1. Surf. temp = 293 K 2. No slip condition 3. Fluxes computed	1. Lapse rate = 6 K km^{-1} starting at 299 K near surface 2. Wind speed = 10 m s^{-1} = geostrophic wind	Parcel method

3. Solutions of the 2TKE Model for Idealized Test Cases

3.1. Case Description

The initial temperature profile consists of a stably stratified column from surface to 3 km height. The potential temperature near the surface is 299 K and the initial lapse rate is 6 K km^{-1}, unless otherwise specified. We present results from our model for two different boundary conditions. The first is a convective boundary layer case called CBL1. In this, we specify a constant surface heat flux of .05 K m s^{-1}. The initial horizontal wind profile is set at a constant value of 10 m s^{-1} over the entire domain and assumed to be the same in magnitude and direction as the geostrophic wind. A constant value of surface friction velocity is prescribed and since the case is highly convective the simulations remain insensitive to this prescription provided it is within certain bounds. This remains the case when the friction velocity is calculated using a surface scheme (Appendix A) assuming a no slip condition. The other case is a stable boundary layer scenario (case: SBL). Here the surface shear (same wind profile as CBL1) drives the turbulence while the surface temperature which is set at 293 K cools and put a cap on the boundary layer growth. The fluxes in this case are computed using the surface scheme as described in Appendix A. Finally, to bring out the properties of the two energies in a pure CBL case, a case similar to CBL1 but with zero mean wind, i.e., a free convective case is employed. In this case, the boundary layer height is calculated using the gradient method (case: CBL2). The cases are summarized in Table 1. No case specific adjustment to the 2TKE model has been made for these different cases. This allows us to understand the capability of the model to adapt these different scenarios.

The simulations are run with a Coriolis parameter of 3.4643×10^{-4} s^{-1}, which is consistent with the Coriolis parameter at 15°. The surface roughness length for momentum and for heat is taken to be the same at 5×10^{-4} m. It is seen that the solutions approach a self-similar state within a large eddy turnover time (of the order of 10 min). The vertical grid size is varied in the range of fine (uniform) grid of size 3 m to coarse grids of size 100 m so as to study the behavior of the solutions as well as that of the different parameters of the model over a range of grid sizes.

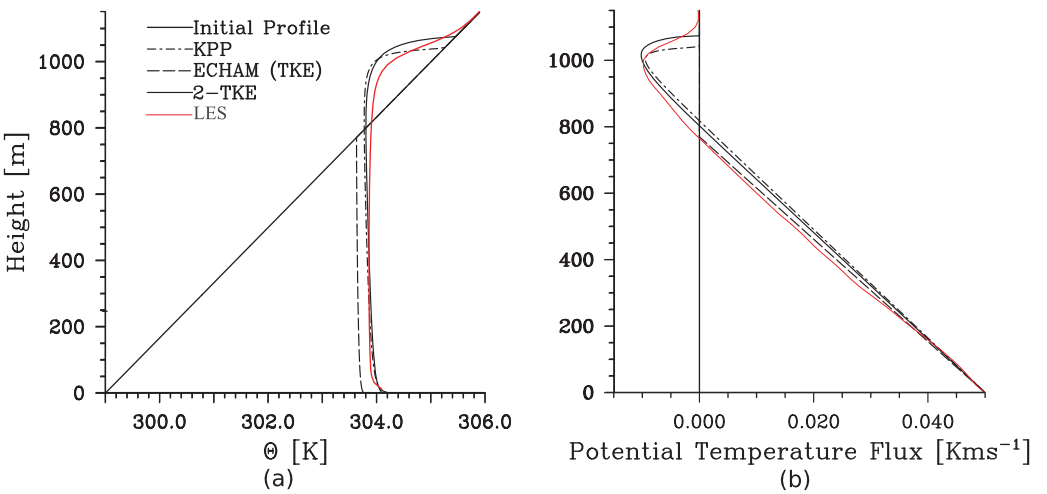

Figure 2. (a) Potential temperature profiles for different models after 10 h and (b) corresponding flux profiles.

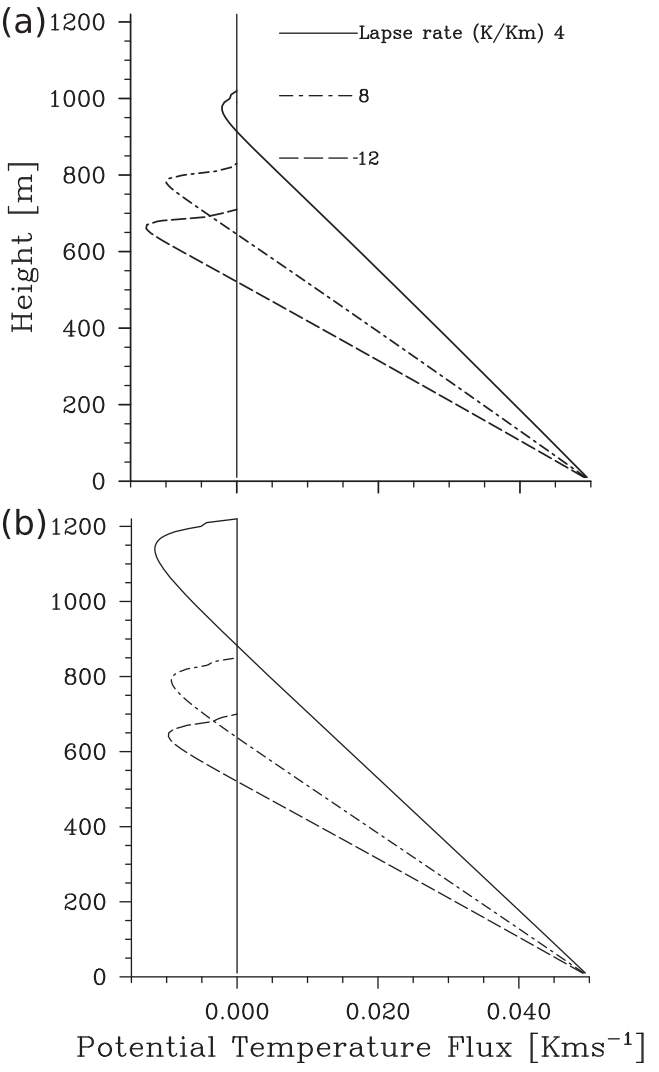

Figure 3. (a) Potential temperature flux profiles for different tropospheric stabilities (formulation not accounting for K_E dependence on the lower tropospheric stability), (b) same as Figure 3a but now taking into account the K_E dependence on lower tropospheric stability.

3.2. Physical Properties

To understand the general properties of the 2TKE model, it has been compared to a simple TKE scheme [*Brinkop and Roeckner*, 1995] implemented in ECHAM6 [*Stevens et al.*, 2013], as well as the *K*-profile parameterization [*Troen and Mahrt*, 1986] for the CBL1 case (Figure 2). In addition, the case simulated in an LES model, the UCLA-LES [*Stevens*, 2010], at very fine resolution (20 m grid size and 3 km domain size in each direction) provides a benchmark solution for the CBL (with solutions presented in the form of statistics averaged over 30 min).

The 2TKE scheme simulates a more realistic representation of the temperature and the flux profiles within the convective boundary layer as compared to the ECHAM scheme and preforms similar to the *K*-profile parameterization (KPP). Its main features are the presence of an unstable surface layer of roughly 15% of the boundary layer height, a well-mixed layer (approximately 60% height) and a stable entrainment zone atop the mixed layer. The ratio of the entrainment flux to the surface flux is governed, among other factors, by the boundary layer height diagnosis method (equation (39)). As has been discussed in previous studies like *Beljaars and Viterbo* [1998], in our model too, it is seen that increasing the critical Richardson number Ri_{cr} and/or the convective excess in the parcel height diagnosis scheme leads to an increase in the entrainment flux vis-a-vis the surface flux. The optimal value for the case of the convective boundary layer for Ri_{cr} is found to be 0.3 and that for the coefficient D used in the excess parcel temperature excess (equation (61)) is found to be 2. Thus (as also shown in *Stevens* [2000]), the structure of the convective boundary layer is well represented and is determined by the shape of the *K*-profile.

Attention should be given to the fact that since all of our used boundary layer schemes are down gradient (refer equation (1)), positive fluxes imply an unstable potential temperature profile. This means that we cannot reproduce counter-gradient fluxes like those we examine in the LES simulations; see *Thomas and Masson* [2006] for example. As an instance, in the LES profiles, from ≈600 to 800 m, the potential temperature profiles are slightly stable even as we note a positive potential temperature flux. Boundary layer models sometimes include a counter-gradient (or a mass flux) component to represent these kinds of counter-gradient fluxes. It is reasoned that the small eddies perform the down-gradient component of the mixing while the large eddies accomplish the counter-gradient mixing. This is usually done ad hoc in models that explicitly recognize just a single scale. Our 2TKE model, recognizing two scales, thus seems like a natural fit to this end. For example, $\bar{e}$, representing the smaller scale of eddies, could be utilized to perform down-

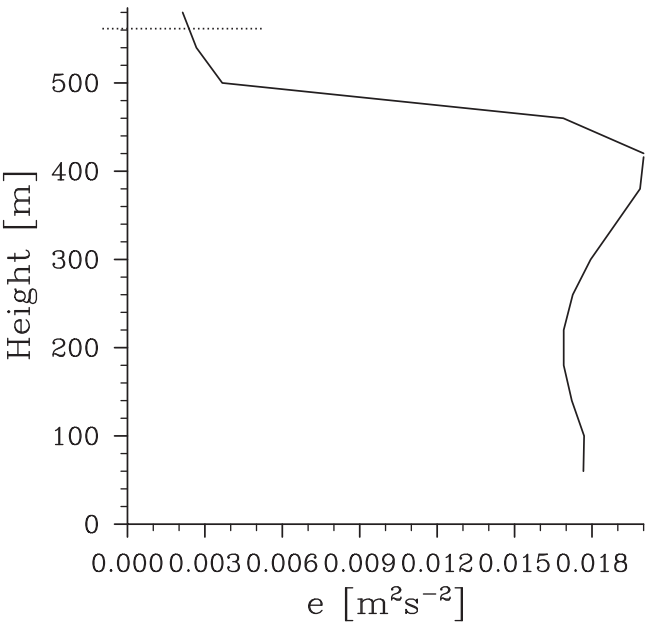

Figure 4. Vertical profile of $\bar{e}$. The dashed line shows the boundary layer height.

gradient mixing while *E*, representing the larger eddies, could be incorporated into the counter-gradient part of the mixing. However, since the present focus is on "scale-adaptivity," we focus on a simple implementation in which both terms are modeled as down gradient.

The shape function (or *K*-profile) used in the present implementation of the 2TKE model is however different from that used in the standard KPP approach, in that instead of a constant shape function, in our model the shape function depends on the free tropospheric lapse rate (section 2.3.2). This helps maintain the correct entrainment ratio (and thus the boundary layer height) irrespective of the stability of the free atmosphere into which the boundary layer deepens. The difference between the standard KPP approach and the approach adopted here can be seen in Figure 3. This figure shows the flux profiles for case CBL2 after 10 h of simulation time for different tropospheric stabilities. Figure 3 shows the case where the exponent *m* in equation (38) is fixed at the value of 2 as in *Troen and Mahrt* [1986]. For this case, it is seen that as the stability of the free troposphere increases the boundary layer growth is not reduced to the appropriate extent. Rather the entrainment rate increases. The increased entrainment rate is consistent with the progressively larger entrainment buoyancy flux. Taking into account the stability of the profiles (as discussed in section 2.3.2) gives a better prediction of the entrainment to surface buoyancy flux ratio (Figure 3b) and consequently the growth of the boundary layer irrespective of the stability above the boundary layer.

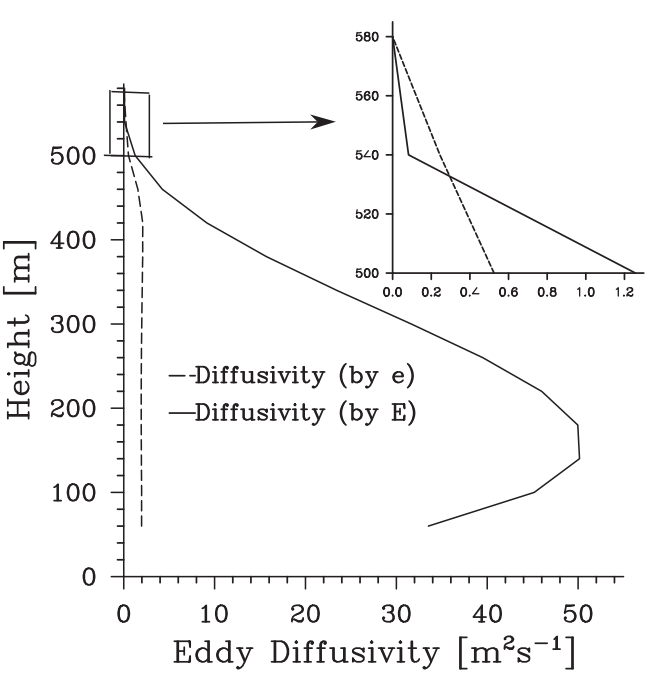

Figure 5. Diffusivity profiles. The inset zooms in near the top of the profiles.

Another novel aspect of the present implementation of the 2TKE model is its representation of mixing in the entrainment zone via two processes. One process is the local mixing of warmer air from the free troposphere into the entrainment zone, and subsequently into the bulk of the boundary layer; and the other is associated with the mixing by warm thermals from the surface penetrating the inversion layer. Figures 4 and 5 show the profile of $\bar{e}$ and the diffusivities through the boundary layer after 3 h for the case CBL2 and a vertical grid size of 40 m. Mixing inside the mixed layer is primarily carried out by *E*. On the other hand in the surface and the entrainment zone, $\bar{e}$ plays a substantial role compared to *E*, and this

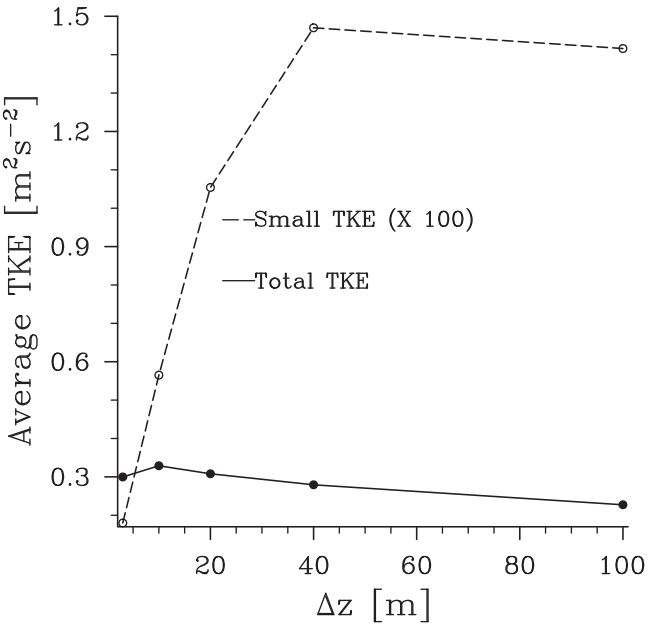

Figure 6. Relative contribution of the large and the small energies across a range of grid sizes.

trend increases as either the top, or the base, of the boundary layer is approached.

3.3. Numerical Properties

As discussed in section 2.4, the development of the 2TKE model has been guided by the desire to maintain a consistent representation of the energetics irrespective of the vertical resolution. This means that E must decrease as the vertical grid spacing becomes larger leading to a compensatory increase in e such that the vertical average (over h) of the sum of the two is approximately constant. Figure 6 shows the vertically averaged sum of the two TKEs as well as the vertically averaged $\bar{e}$ across a range of grid sizes. Up until a certain grid size, the sum is very nearly constant, beyond which numerical effects reduce the sum of the two energies as a whole (nonetheless the ratio of the averaged $\bar{e}$ to the total is seen to increase with increasing grid sizes).

Through the consistent representation of the distribution of energy between E and $\bar{e}$ and the employing of $\bar{e}$ to represent the entrainment process, we compensate for the numerical artifacts arising from poor vertical resolution. Figure 7 which compares the simulated boundary layer depths after 3 h of simulation time from KPP and 2TKE model upon the usage of different vertical grid sizes helps illustrate this. Even with relatively coarse vertical grid spacing, the 2TKE simulated boundary layer depth stays closer to the value when finer grids are employed: a property distinctly different from the KPP scheme.

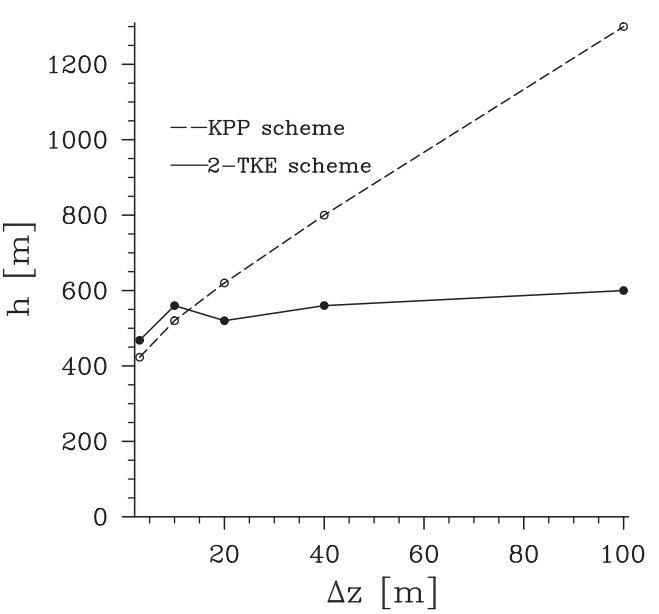

Figure 7. Boundary layer height predicted by the KPP and the 2TKE model for a range of grid sizes.

3.4. Behavior Across Regimes

Next we explore the behavior of the 2TKE model in the stable boundary layer limit. A vertical grid spacing of 10 m has been employed for these simulations. In the stable boundary layer, the turbulence that sustains the boundary layer is generated by the balance of production (via local shear) and destruction (via buoyancy). Here the TKE model performs reasonably well as compared to the KPP which has been designed more specifically for convective scenarios (not shown). The 2TKE model also performs according to theory (Figure 8a, case SBL; the theory of idealized stable boundary layers is discussed in the Appendix A). This is identified by the presence of inversions at the surface and the boundary layer top as well as an approximately correct growth rate and

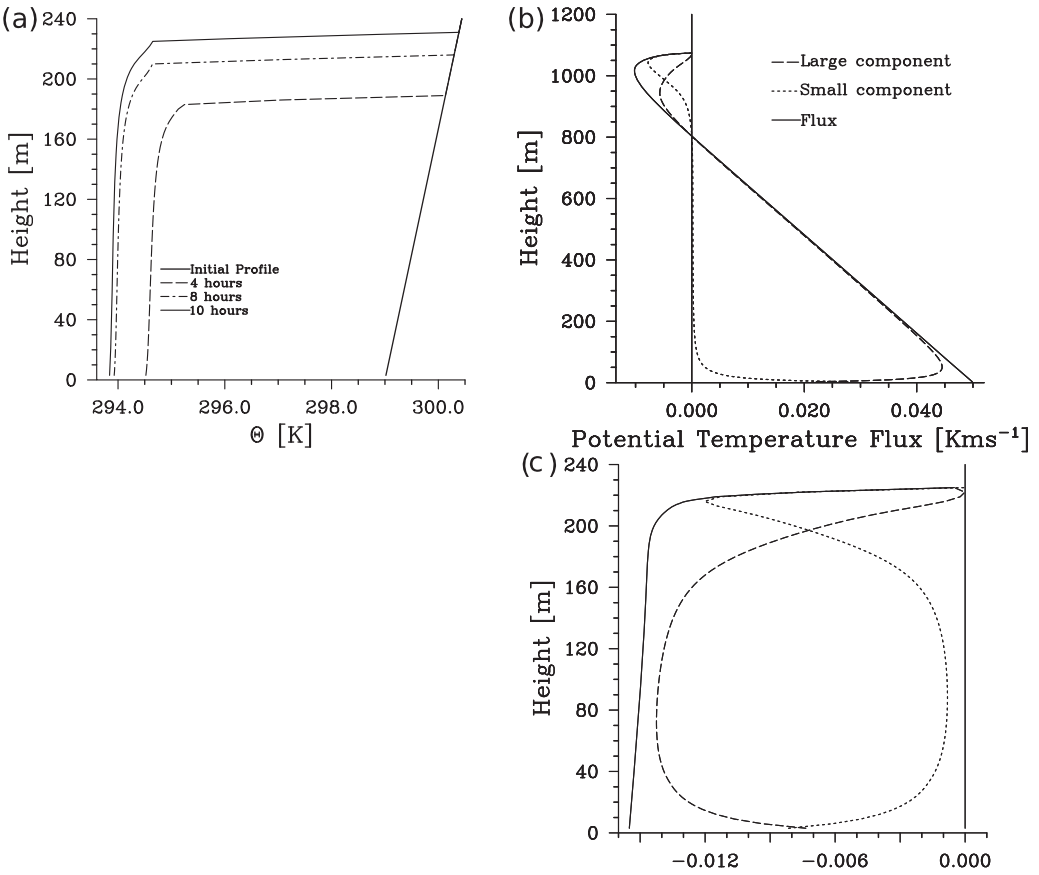

Figure 8. (a) Boundary layer growth for case: SBL. (b) The flux contribution from the large and small scales for case CBL1. (c) The same for SBL.

the equilibrium height of the layer. The major property of the 2TKE scheme that we want to highlight in this section is its ability to emphasize the mixing contributions of E or $\bar{e}$ depending on the type of eddies that perform the mixing in a given scenario. Thus in a convective case (CBL2) where the boundary layer develops as a result of convective thermals driven by surface buoyancy, the large-scale fluxes (represented by E) dominate the mixed layer and the small-scale fluxes play a significant role only at the surface and the entrainment zone (Figure 8b). On the other hand, in the stable boundary layer case, the small-grid-scale fluxes, associated with the small-scale energy, $\bar{e}$ play a more important role throughout the boundary layer (Figure 8c).

4. Conclusions

A new boundary layer scheme called the 2TKE model has been presented. Its distinguishing feature is to solve for two turbulence kinetic energies linked via the turbulence energy cascade. Our approach is the division of scales in PBL turbulence into two parts: eddies or circulations that range from the scale of the model vertical grid to the depth of the boundary layer and eddies that are subgrid relative to the vertical grid scale. The model is derived from the full set of LES equations (which set the limit for the smaller scales) formulated in terms of a subgrid (or *Deardorff*) TKE and is shown to reduce (modulo the treatment of the horizontal fluxes) to these equations in the limit of the grid spacing, Δx, being much less than the depth of the boundary layer. In the large-scale limit (i.e., $\Delta x > h$), we have tested the model for idealized cases in a single-column setup and it is seen that it represents the boundary layer as well as the parameterizations, that are widely used, and much better than the current parameterization used in ECHAM. A key reason for the development of the model is the rationalization that a model working in these two limits of horizontal grid sizes can be tuned to work in the "grey zone": an idea we explore in the companion paper (Bhattacharya and Stevens, submitted manuscript, 2015).

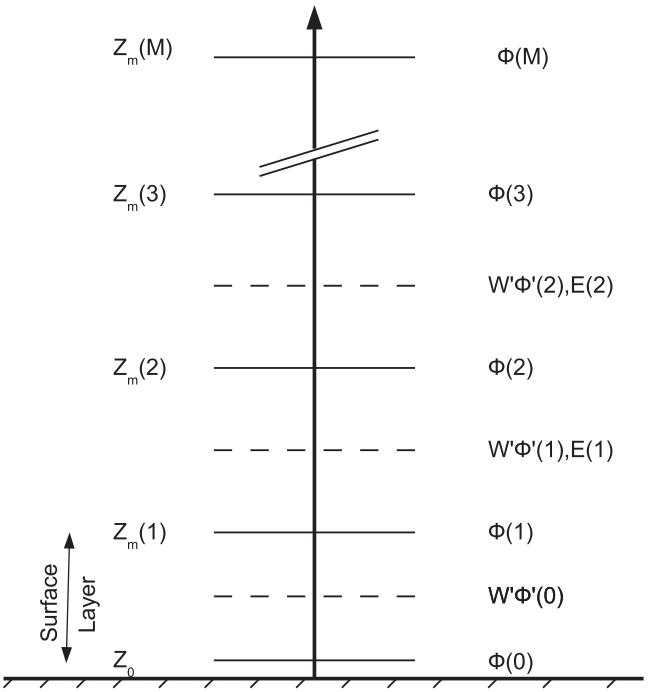

Figure 9. Single-column grid.

An advantage of the 2TKE model is the combination of the *local* and the *nonlocal* approaches to boundary layer modeling through the use of two turbulence kinetic energies: one representing the energy on scales smaller than Δz, called the small-scale energy, $\bar{e}$ and the other over scales that range from $\min(h, \Delta x)$ to Δz (assuming of course that $\Delta z \leq \Delta x$), called the large-scale energy, E. We therefore formulate length scales over which these two energies mix and dissipate. The mixing length of the small-scale energy has been defined in such a way that the small-scale energy contributes substantially to the mixing inside the entrainment zone of the CBL. The mixing length of the large-scale energy takes into account the boundary layer height, the free tropospheric stability (both included in a shape function that roughly indicates the size of the largest eddy contributing to mixing at a given height) and the fact that in the entrainment zone, the small-scale energy is responsible for much of the mixing. The dissipation length scale of small energy is proportional to the vertical grid size of the model while that for the large energy is defined in such a way that the total energy is consistently represented irrespective of the grid size of the host model. These choices lead to a model of the boundary layer that behaves reasonably well across a range of vertical grid sizes. An extra advantage of the usage of two energies is the smooth transition of the representation of the boundary layer from convective to stable scenarios, with the small-scale energy contributing more in the stable scenario.

Because we initially sought to identify the key issues in modeling the boundary layer and utilizes them to design the 2TKE model aiming at scale-adaptivity, the simple case of a dry boundary layer has been explored. In the climate system, however, cloud-topped boundary layers are of paramount importance. The 2TKE model provides the two scales necessary to better couple the scales present in the subcloud layer to the ones present in the cloud layer and should be explored as the next step.

Appendix A: Single-Column Model

This section describes the off-line implementation (or single-column model) that has been developed to test the 2TKE model. The different types of boundary condition used to explore its properties are explained.

A1. Grid

The implementation of the 2TKE model is on a one-dimensional vertical grid which discretizes the vertical height coordinate, z (Figure 9). M is the number of model levels. In this, the first level is always assumed to lie within the surface layer and hence a logarithmic distribution of the model variables, following Monin-Obukhov theory, is adopted. Above the first level, a linear profile is assumed as an initial condition. The solid horizontal lines are the model full-levels, where the model variable values, $\bar{u}, \bar{v}, \bar{\theta}$, are specified, while the dashed horizontal lines represent the half-levels, where the fluxes and hence the diffusivities as well as the two TKEs, $\bar{e}$ and E, are defined. Specifying the variables in this manner simplifies the spatial discretization.

The nonlinear diffusion equation, describes the evolution of the potential temperature, can be written as

$$\frac{\partial\bar{\theta}}{\partial t}=-\frac{\partial\overline{\theta' w'}}{\partial z}=\frac{\partial}{\partial z}\left(K_h\frac{\partial\bar{\theta}}{\partial z}\right). \tag{A1}$$

K_h includes the contribution from both scale of eddies (the distinction makes no difference for the numerical scheme). This is solved using second-order central differencing in space and semiimplicit time differencing (Φ being a generic mean variable).

$$\frac{{\Phi_i}^{n+1}-{\Phi_i}^{n}}{\Delta t}=\frac{(K_{i+1/2}\ (\frac{{\Phi_{i+1}}^{n+1}-{\Phi_i}^{n+1}}{\Delta z_{i+1}})-K_{i-1/2}(\frac{{\Phi_i}^{n+1}-{\Phi_{i-1}}^{n+1}}{\Delta z_i}))}{\frac{1}{2}(\Delta z_{i+1}+\Delta z_i)}. \tag{A2}$$

Here the superscript n denotes the time level and subscript i denotes the height level.

A2. Boundary Conditions

The surface fluxes of buoyancy and momentum are the boundary conditions to the model (the fluxes at the top of the domain are assumed to be zero). Two types of surface flux formulations have been employed to bring out the properties of our scheme. In the first, a constant surface flux is specified. This helps in comparing the model solutions to the theoretical solutions as well as in tuning model parameters. The other is the specification of constant surface temperature at the surface (velocity being zero there) and calculating the fluxes from the difference between values at the surface and values at the first model level. This is a more realistic boundary condition since it limits the heat uptake by the boundary layer and helps in quantifying the interaction between the surface scheme and the boundary layer scheme. The fluxes are calculated following a bulk approach, such that

$$\overline{w'\Phi'}(0)=-C_\Phi|v(1)|(\bar{\Phi}(1)-\bar{\Phi}(0)). \tag{A3}$$

Here $V(1)$ is the wind speed at the first model level and C_ϕ is the transfer coefficient which is calculated from Monin-Obukhov similarity theory.

The transfer coefficient (C_ϕ) in the surface layer is obtained from the Monin-Obukhov similarity theory by integrating the flux profile over the lowest model level, following the analytical expressions derived by *Louis* [1979] for momentum and heat (and other scalars). The process involves computing a "neutral" transfer coefficient as a function of the surface properties and then modifying it based on the stability of the surface layer.

A3. Theoretical Growth of the Boundary Layer Depth

We briefly discuss the theoretical growth of the boundary layer provided it grows into an atmosphere with fixed lapse rate. Details can be found in *Garratt* [1992]. For a convective boundary layer (assuming the flux at the top is a constant fraction of the surface flux):

$$h^2(t_1)\ \propto\ 2\frac{\int_0^{t_1}\overline{w'\theta'}_0 dt}{G}, \tag{A4}$$

where G is the stability of the layer into which the boundary layer grows.

For a stable boundary layer, a steady state height is governed mainly by the shear-generated growth of the turbulent structures, so that

$$h_e=\gamma_c\sqrt{u_* L/|f|}. \tag{A5}$$

γ_c is a constant which is obtained from the balance of shear production of turbulence and the buoyant destruction of turbulence in steady state. For horizontal terrain, γ_c is taken to be 0.4 and u_* is the surface friction velocity, L is the Monin-Obukhov length, and f is the Coriolis frequency. Since the surface friction velocity and hence the Monin-Obukhov length scale varies as the profile changes in time, an average value is taken to provide a rough estimate of h_e. The evolution of the boundary layer height with respect to time is governed by

$$\frac{\partial h}{\partial t}=\frac{(h_e-h)}{T_{\text{relax}}}, \tag{A6}$$

with h being the instantaneous boundary layer height and T_{relax} is the relaxation time which is given by the difference between the potential temperature of the surface and the top of the stable layer divided by the

surface cooling rate. The solution to the relaxation equation is a logarithmic growth of h with time, eventually reaching h_e on the timescale of T_{relax}.

Acknowledgments
We would like to thank the Deutscher Wetterdienst (DWD) for providing support for the project. The authors would also like to thank C. Hohenegger and A. Siefert for valuable suggestions. Thanks are in order to A. Dipankar and Chiel Van Heerwaarden for some thought provoking discussions on the topic.

References

Baldauf, M., et al. (2011), Operational convective-scale numerical weather prediction with the COSMO model: Description and sensitivities, *Mon. Weather Rev.*, *139*, 3887–3905, doi:10.1175/MWR-D-10-05013.1.

Beljaars, A., and P. Viterbo (1998), The role of the boundary layer in a Numerical Weather Prediction model, in *Clear and Cloudy Boundary Layers*, edited by A. Holtslag and P. G. Duynkerke, Royal Netherlands Academy of Arts and Sciences, North-Holland, pp. 287–304.

Blackadar, A. K. (1962), The vertical distribution of wind and turbulent exchange in a neutral atmosphere, *J. Geophys. Res.*, *67*(8), 3095–3102.

Bougeault, P. (1981a), Modeling the trade-wind cumulus boundary layer. Part I: Testing the ensemble cloud relations against numerical data, *J. Atmos. Sci.*, *38*, 2414–2428.

Bougeault, P. (1981b), Modeling the trade-wind cumulus boundary layer. Part II: A higher-order one-dimensional model, *J. Atmos. Sci.*, *38*, 2414–2428.

Bretherton, C. S., and S. Park (2009), A new moist turbulence parameterization in the Community Atmosphere Model, *J. Clim.*, *22*(12), 3422–3448, doi:10.1175/2008JCLI2556.1.

Brinkop, S., and E. Roeckner (1995), Sensitivity of a general circulation model to parameterizations of cloud-turbulence interactions in the atmospheric boundary layer, *Tellus, Ser. A*, *47*, 197–220.

Deardorff, J. (1974), Three-dimensional numerical study of the height and mean structure of a heated planetary boundary layer, *Boundary Layer Meteorol.*, *7*, 81–106.

Deardorff, J. W. (1970), Preliminary results from numerical integrations of the unstable planetary boundary layer, *J. Atmos. Sci.*, *27*, 1209–1211.

Deardorff, J. W. (1980), Stratocumulus-capped mixed layers derived from a three-dimensional model, *Boundary Layer Meteorol.*, *18*, 495–527.

Dyer, A. (1974), A review of flux-profile relationships, *Boundary Layer Meteorol.*, *7*, 363–372.

Finger, J., and P. Wendling (1990), Turbulence structure of Arctic stratus clouds derived from measurements and calculations, *J. Atmos. Sci.*, *47*(11), 1351–1373.

Garratt, J. R. (1992), The Atmospheric Boundary Layer, *Cambridge Atmos. Space Sci. Ser.*, Cambridge University Press.

Golaz, J.-C., V. E. Learson, and W. R. Cotton (2002a), A PDF based model for boundary layer clouds. Part I: Method and Model description, *J. Atmos. Sci.*, *59*, 3540–3551.

Golaz, J.-C., V. E. Learson, and W. R. Cotton (2002b), A PDF based model for boundary layer clouds. Part II: Model results, *J. Atmos. Sci.*, *59*, 3552–3571.

Grenier, H., and C. S. Bretherton (2001), A moist PBL parameterization for large-scale models and its application to subtropical cloud-topped marine boundary layers, *Mon. Weather Rev.*, *129*, 357–377.

Högström, U. (1988), Non-dimensional wind and temperature profiles in the atmospheric surface layer: A re-evaluation, *Boundary Layer Meteorol.*, *42*, 55–78.

Honnert, R., V. Masson, and F. Couvreux (2011), A diagnostic for evaluating the representation of turbulence in atmospheric models at the kilometric scale, *J. Atmos. Sci.*, *68*(12), 3112–3131, doi:10.1175/JAS-D-11-061.1.

Kolmogorov, A. (1991), The local structure of turbulence in incompressible viscous fluid for very large Reynolds numbers, *Proc. R. Soc. London, Ser. A*, *434*, 9–13.

Lappen, C. L., and D. A. Randall (2001a), Toward a unified parameterization of the boundary layer and moist convection. Part I: A new type of mass-flux model, *J. Atmos. Sci.*, *58*, 2021–2036.

Lappen, C. L., and D. A. Randall (2001b), Toward a unified parameterization of the boundary layer and moist convection. Part II: Lateral mass exchanges and subplume-scale fluxes, *J. Atmos. Sci.*, *58*, 2037–2051.

Lappen, C. L., and D. A. Randall (2001c), Toward a unified parameterization of the boundary layer and moist convection. Part II: Simulations of clear and cloudy convection, *J. Atmos. Sci.*, *58*, 2052–2072.

Large, W., J. Mcwilliams, and S. Doney (1994), Oceanic vertical mixing: A review and a model with a nonlocal boundary layer parameterization, *Rev. Geophys.*, *32*(94), 363–403.

Lock, A., A. Brown, M. Bush, and G. Martin (2000), A new boundary layer mixing scheme. Part I: Scheme description and single-column model tests, *Mon. Weather Rev.*, *128*(1998), 3187–3199.

Louis, J.-F. (1979), A parametric model of vertical eddy fluxes in the atmosphere, *Boundary Layer Meteorol.*, *17*, 187–202.

Mellado, J. P., B. Stevens, and H. Schmidt (2014), Wind shear and buoyancy reversal at the stratocumulus top, *J. Atmos. Sci.*, *71*, 1040–1057, doi:10.1175/JAS-D-13-0189.1.

Mellor, G. L., and T. Yamada (1974), A hierarchy of Turbulence Closure Models for planetary boundary layers, *J. Atmos. Sci.*, *31*, 1791–1805.

Rotta, J. (1951), Statistische Theorie nichthomogener Turbulenz, *Z. Phys.*, *129*(6), 547–572, doi:10.1007/BF01330059.

Siebesma, A. P., P. M. M. Soares, and J. Teixeira (2007), A Combined eddy-diffusivity mass-flux approach for the convective boundary layer, *J. Atmos. Sci.*, *64*(4), 1230–1248, doi:10.1175/JAS3888.1.

Stevens, B. (2000), Quasi-steady analysis of a PBL model with an eddy-diffusivity profile and nonlocal fluxes, *Mon. Weather Rev.*, *128*, 824–836.

Stevens, B. (2010), *Introduction to UCLA-LES*. [Available at http://www.mpimet.mpg.de/fileadmin/atmosphaere/herz/les_doc.pdf.]

Stevens, B., et al. (2013), The atmospheric component of the MPI-M Earth System Model: ECHAM6, *J. Adv. Model. Earth Syst.*, *5*, 146–172, doi:10.1002/jame20015.

Sullivan, P. P., and E. G. Patton (2011), The effect of mesh resolution on convective boundary layer statistics and structures generated by large-eddy simulation, *J. Atmos. Sci.*, *68*, 2395–2415, doi:10.1175/JAS-D-10-05010.1.

Thomas, S., and V. Masson (2006), A parameterization of third-order moments for the dry convective boundary layer, *Boundary Layer Meteorol.*, *120*, 437–454.

Tiedke, M. (1989), A comprehensive mass flux scheme for cumulus parameterization in large-scale models, *Mon. Weather Rev.*, *117*(8), 1779–1800.

Troen, I., and L. Mahrt (1986), A simple model of the atmospheric boundary layer; sensitivity to surface evaporation, *Boundary Layer Meteorol.*, *37*(I), 129–148.

Wyngaard, J. C. (2004), Toward numerical modeling in the "Terra Incognita," *J. Atmos. Sci.*, *61*(14), 1816–1826, doi:10.1175/1520-0469(2004)061 < 1816:TNMITT>2.0.CO;2.

Zhang, D.-L., and W.-Z. Zheng (2004), Diurnal cycles of surface winds and temperatures as simulated by five boundary layer parameterizations, *J. Appl. Meteorol.*, *43*, 157–169.